Journal of Molecular Structure 1072 (2014) 84–93

Contents lists available at ScienceDirect

Journal of Molecular Structure

journal homepage: www.elsevier.com/locate/molstruc

Synthesis and structural characterization of (*E*)-*N*′-((Pyridin-2-yl)methylene) benzohydrazide by X-ray diffraction, FT-IR, FT-Raman and DFT methods

N. Ramesh Babu [a], S. Subashchandrabose [b], M. Syed Ali Padusha [c], H. Saleem [d,*], V. Manivannan [e], Y. Erdoğdu [f]

[a] Dept. of Physics, M.I.E.T. Engineering College, Trichy 620007, Tamil Nadu, India
[b] Dept. of Physics, M.A.R. College of Engineering & Technology, Trichy 621316, Tamil Nadu, India
[c] PG and Research Dept. of Chemistry, Jamal Mohamad College (Autonomous), Trichy 620020, Tamil Nadu, India
[d] Dept. of Physics, Annamalai University, Annamalai Nagar 608002, Tamil Nadu, India
[e] Dept. of Research and Development, PRIST University, Vallam, Thanjavur 613403, Tamil Nadu, India
[f] Dept. of Physics, Ahi Evran University, Kirsehir 40040, Turkey

HIGHLIGHTS

- Synthesis of (*E*)-*N*[1]-((Pyridin-2-yl) methylene) benzohydrazide (PMBH).
- A vibrational analysis by FT-IR, FT-Raman and TED.
- The crystal structure of the compound analyzed.
- The band gap energy is studied using HOMO and LUMO.
- Molecular electrostatic potential of PMBH was carried out.

GRAPHICAL ABSTRACT

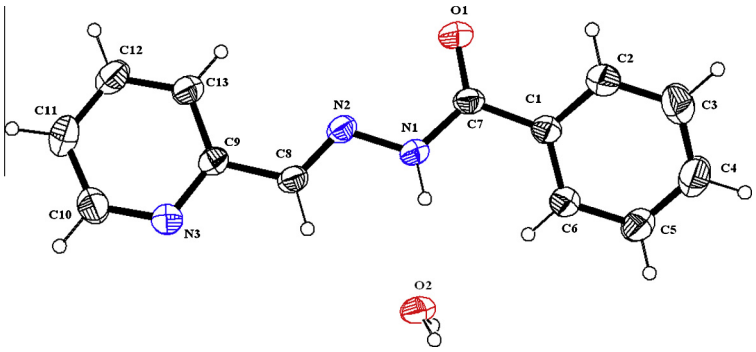

ARTICLE INFO

Article history:
Received 9 February 2014
Received in revised form 17 April 2014
Accepted 17 April 2014
Available online 29 April 2014

Keywords:
FT-IR
FT-Raman
TED
NBO
MEP

ABSTRACT

The (*E*)-*N*′-((Pyridin-2-yl)methylene)benzohydrazide (PMBH) was synthesized and its structural characterization was made by the X-ray diffraction method. The spectral investigations such as FT-IR, FT-Raman and UV–Visible spectra were carried out. The recorded X-ray diffraction bond parameters were compared with theoretical values calculated at B3LYP/6-311++G (d, p) level of theory. The observed spectral results were compared with the computed wavenumber. The vibrational assignments were carried out by the total energy distribution (TED) method. The first order hyperpolarizability, intra-molecular charge transfer and band gap energy were studied using B3LYP/6-311++G (d, p) calculation. The electronic transition was studied using UV–Visible spectrum and the observed values were compared with the theoretical values. The electrostatic potential surface of the title molecule was also analyzed using the same level of basis set.

Introduction

The hydrazone group in the organic molecule brings out several physical and chemical properties. The hydrazones are bearing the

* Corresponding author. Mobile: +91 9443879295.
E-mail addresses: sscbphysics@gmail.com, nrbmiet@gmail.com (H. Saleem).

http://dx.doi.org/10.1016/j.molstruc.2014.04.060
0022-2860/

>C=N—N< which leads the molecule towards nucleophilic and electrophilic in nature. In the hydrazone moiety, the nitrogen atom behaves as nucleophilic and carbon atom behaves as nucleophilic as well as electrophilic in nature [1–3]. The ability of hydrazones to react with both electrophilic and nucleophilic reagents widens their application in organic chemistry and designing the new drugs [1,4,5]. Several hydrazone derivatives have been reported as insecticides, nematicides, herbicides, rodenticides and antituberculosis in addition to that some of the hydrazone were found to be active against leukemia, sarcoma and illnesses [5,6]. The two types of photochemical reactions such as nitrogen–nitrogen bond cleavage and hydrogen migration from nitrogen to carbon were described for hydrazone [7,8]. The hydrazones were also shown to be involved in bio-molecular reactions such as cycloadditions and condensations [1,4]. The benzohydrazide derivatives shows wide spectrum of biological activities such as antibacterial [9], antifungal [10], antitubercular [11], and antiproliferative [12] activities. Total energy distribution (TED) calculation, which show the relative contributions of the redundant internal coordinates to each normal vibrational mode of the molecule and thus enable us numerically to describe the character of each mode using scaled quantum mechanical (SQM) program. In the present study, (*E*)-*N*′-((Pyridin-2-yl) methylene)benzohydrazide (PMBH) molecule was synthesized and its structure was investigated by X-ray diffraction method and the spectral characterizations were made by FT-IR, FT-Raman and UV–Visible spectra and the corresponding theoretical predictions were carried out by using B3LYP/6-311++G (d, p) level of calculation.

Experimental details

Preparation of Schiff base

The 2.4 ml (0.025 mol) ethanolic solution of Pyridin-2-carboxaldehyde was added with (0.025 mol) 3.4 g of benzohydrazide (BH). The reaction mixture was taken in a round bottom flask and kept over a magnetic stirrer and stirred well in ice cold condition for 2 h. The colorless precipitate obtained was filtered and dried over vacuum.

Crystal structure determination and refinement

The crystal structure determination was carried out by X-ray diffraction analysis and the approximate dimension of the crystal was about 0.25 × 0.20 × 0.20 mm^3. The measurements were performed on a Bruker Apex II CCD diffractometer which is carried out from the SAIF Laboratory, IIT(M), Tamilnadu, India. The intensity data were collected using graphite monochromated Mo Kα radiation (λ = 0.71073 Å). The structure was solved by direct method and refined by full matrix least – squares against F^2 for all data using SHELXL97 software [13]. All non-hydrogen atoms in the compound were anisotropically refined. The hydrogen atoms were positioned geometrically and refined using riding model with C—H = 0.93 Å and U_{iso} (H) = 1.2 U_{eq} (C) for aromatic C–H, N–H = 0.86 Å and U_{iso} (H) = 1.2 U_{eq} (C) for N—H, OH distance restrained to 0.82 Å and U_{iso} (H) = 1.2 U_{eq} (C) for O—H.

Data collection: *APEX2*; Cell refinement: *SAINT*; data reduction: *SAINT* [14]; program(s) used to solve structure: *SHELXS97*; program(s) used to refine structure: *SHELXL97* [13], molecular graphics: *PLATON* [15]; software used to prepare material for publication: *SHELXL97*. The crystallographic data and details of the refinement process are given in Table 1 and the refined crystal structure was shown in Fig. 1a.

FT-IR, FT-Raman and UV–Visible details

The FT-IR spectrum of PMBH was recorded in the region of 400–4000 cm^{-1} on an IFS 66 V spectrophotometer using the KBr pellet technique. The spectrum was recorded in room temperature with a scanning speed of 10 cm^{-1} per minute at the spectral resolution of 2.0 cm^{-1}. The FT-Raman spectrum of the title compound was recorded by using the 1064 nm line of a Nd:YAG laser as an excitation wavelength in the region of 50–3500 cm^{-1} on Bruker model IFS 66 V spectrophotometer equipped with an FRA 106 FT-Raman module accessory at the spectral resolution of 4 cm^{-1}. The ultraviolet absorption spectrum of PMBH was recorded in the range of 200–500 nm by using a Perkin Elmer Lambda-35 spectrometer and UV pattern was taken from a 10^{-5} molar solution of PMBH dissolved in methanol.

Table 1
Crystallographic data collection and refinement parameters for PMBH.

Parameters	
Crystal data	
Chemical formula	$C_{13}H_{13}N_3O_2$
Mr	243.26
Crystal system, space group	Orthorhombic, *Pbca*
Temperature (K)	295
a, *b*, *c* (Å)	7.141(5), 11.984(5), 29.499(5)
V(Å^3)	2524 (2)
Z	8
Radiation type	0.09
Crystal size (mm)	0.25 × 0.20 × 0.20
Data collection	
Diffractometer	Bruker Apex II CCD diffractometer
Absorption correction	Multi-scan *SADABS*[a]
T_{min}, T_{max}	0.978, 0.985
No. of measured, independent and observed [$I > 2\alpha(I)$] reflection	15,054, 3163, 1780
R_{int}	0.036
$(sin\ \theta/\lambda)_{max}$ (Å^{-1})	0.669
Refinement	
$R[F^2 > 2\alpha(F^2)]$, $wR(F^2)$, *S*	0.045, 0.126, 1.00
No. of reflections	3163
No. of parameters	170
No. of restrains	2
H-atom treatment	H atoms treated by a mixture of independent and constrained refinement
$\Delta\rho_{max}$, $\Delta\rho_{min}$ (e Å^{-3})	0.14, −0.17

[a] SADABS,- G.M. Sheldrick, University of G/" Ottingen, Germenay (1996).

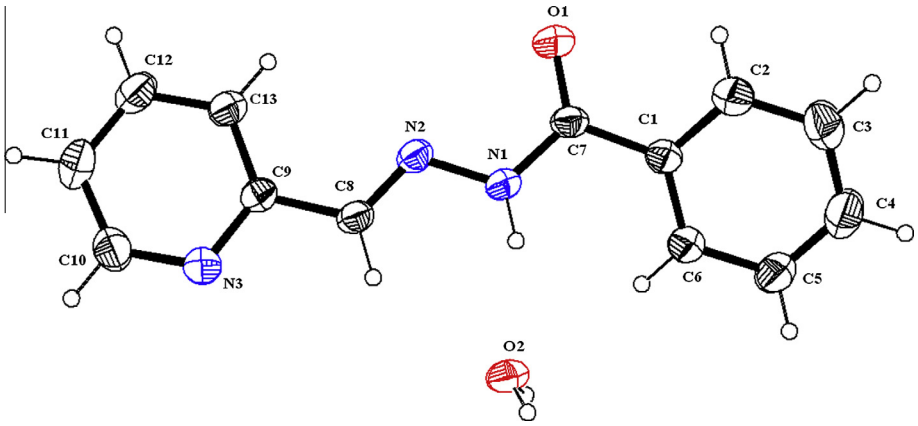

Fig. 1a. The X-ray diffraction structure of (*E*)-*N*′-((Pyridin-2-yl) methylene) benzohydrazide monohydrate.

Computational details

In order to establish the stable possible conformers, the conformational space of PMBH compound was scanned with molecular mechanic simulations. For meeting the requirements of accuracy and computing economy, theoretical methods and basis sets were considered. The Density Functional Theory (DFT) has been proved to be extremely useful in treating electronic structure of molecules. The entire calculations were performed at B3LYP/6-311++G (d, p) level of basis set using Gaussian 03W [16] program package, invoking gradient geometry optimization [16,17]. The optimized structural parameters were used in the vibrational frequency calculations at the DFT level to characterize all the stationary points as minima. The vibrationaly averaged nuclear positions of PMBH were used for harmonic vibrational frequency calculations resulting in IR and Raman frequencies together with intensities and Raman depolarization ratios. The vibrational modes were assigned on the basis of TED analysis using the Scaled quantum mechanical program [18].

The Raman activity was calculated by using Gaussian 03W package and the activity was transformed into Raman intensity using Raint program [19] by the expression:

$$I_i = 10^{-12} \times (\nu_0 - \nu_i)^4 \times \frac{1}{\nu_i} \times RA_i \quad (1)$$

where I_i is the Raman intensity, RA_i is the Raman scattering activity, ν_i is the wavenumber of the normal modes and ν_0 denotes the wavenumber of the excitation laser [20].

Results and discussion

Molecular geometry

The molecule (*E*)-*N*′-((Pyridin-2-yl)methylene) benzohydrazide (PMBH) was synthesized and characterized by X-ray diffraction method. The optimization of PMBH was carried out by using B3LYP/6-311++G (d, p) level of calculation. The title molecule consists of pyridin and phenyl ring fused by hydrazone linkage. In PMBH the hydrazone linkage plays an important role. For the carbonyl (C_{16}═O_{17}) group bond length in hydrazone link was observed at 1.224 Å whereas the calculated bond length was about 1.212 Å. The bond length of >C_{11}═N_{13}< group was observed at 1.266 Å, whereas it was computed about 1.279 Å. The bond N_{14}—N_{13} behaves as a bridge between the phenyl and pyridin ring. The bond length of N_{14}—N_{13} was observed at 1.375 Å and calculated value as 1.353 Å. Similarly the bond length of C_{16}—N_{14} is about 1.354 Å and 1.391 Å as observed and calculated values respectively. The results obtained by the X-ray diffraction method were comparable with computed molecular geometry of the title compound. The rest of the observed and calculated bond lengths for phenyl and pyridin rings coincided with one and each other with few exceptions. The bond angle of O_{17}—C_{16}—C_{18} is observed at 121.48°, which is in consistent with calculated value of 122.79° and also finds support from Bikas et al. [21]. In hydrazone linkage, the angle for C_{11}═N_{13}—N_{14} was calculated about 117.41° whereas the observed value is 116.43°. The bond angle of C═N—C link 117.41° is in line with literature values [22,23]. The carbonyl group makes the angle with hydrazone link is about 114.11° and slightly deviated from the observed value. This bond angle finds support from literature [23,24]. The bond angle calculated between pyridin and hydrazone link (C_1—C_{11}═N_{13}) is about 121.42° which is in line with the observed X-ray data 121.34°.

In the title compound ($C_{13}H_{11}N_3O$) the pyridin ring makes a dihedral angle of 28.27°(6) with the phenyl ring and molecules are linked through weak C—H···π interaction. The dihedral angles calculated for C_1—C_{11}—N_{13}—N_{14}, C_{11}—N_{13}—N_{14}—C_{16} and N_{13}—N_{14}—C_{16}—C_{18} are −179.32°, −175.09° and −177.60° in agreement with experimentally observed results and also coincide with literature values [21,22]. Most of the calculated bond parameters using B3LYP/6-311++G (d, p) were agreeable with X-ray diffraction values. The geometric parameter of the title molecule agrees well with the reported similar structure [25,26]. The recorded and calculated bond parameters were listed in Table 2. The optimized molecular structure of the title compound is shown in Fig. 1b.

Vibrational assignments

The title molecule belongs to C_1 point group symmetry. It consists of 28 atoms which undergoes 78 normal modes of vibrations. In this 53 modes of vibrations are in-plane and remaining 25 are out-of-plane vibrations. The PMBH was characterized by FT-IR and FT-Raman vibrational spectra. The vibrational study of the molecule was carried out by using B3LYP/6-311++G (d, p) level of theory. The recorded and calculated spectral results were compared and assigned to the corresponding modes of vibrations. For accurate vibrational assignment the total energy distribution analysis was performed by scaled quantum mechanical calculation (SQM). The recorded and predicted spectral results were given in Table 3. The combined vibrational spectra of PMBH were shown in Fig. 2 (FT-IR) and Fig. 3 (FT-Raman).

N—H Vibrations

The N—H stretching vibration occurs in the region of 3300–3500 cm^{-1} [27]. The hetero aromatic molecule containing N—H

Table 2
The observed and calculated bond parameters of PMBH.

Parameters Bond length (Å)	Cal.[a]	X-ray[b]	Parameters Bond angle (°)	Cal.[a]	X-ray[b]	Parameters Bond angle (°)	Cal.[a]	X-ray[b]
C1—C2	1.403	1.384	C2—C1—N6	122.84	122.05	C18—C19—C21	120.31	120.21
C1—N6	1.344	1.334	C2—C1—C11	122.21	122.49	C18—C19—H22	120.67	119.9
C1—C11	1.468	1.462	N6—C1—C11	114.96	114.95	C21—C19—H22	118.98	119.9
C2—C3	1.387	1.371	C1—C2—C3	118.45	119.37	C18—C20—C23	120.35	120.50
C2—H8	1.083	0.930	C1—C2—H8	119.49	120.3	C18—C20—H24	118.58	119.7
C3—C4	1.395	1.368	C3—C2—H8	122.06	120.3	C23—C20—H24	121.07	119.7
C3—H7	1.084	0.930	C2—C3—C4	119.03	118.91	C19—C21—C25	120.07	120.25
C4—C5	1.393	1.368	C2—C3—H7	120.35	120.5	C19—C21—H26	119.77	119.9
C4—H9	1.083	0.930	C4—C3—H7	120.62	120.5	C25—C21—H26	120.15	119.9
C5—N6	1.335	1.337	C3—C4—C5	118.30	118.58	C20—C23—C25	120.14	120.72
C5—H10	1.086	0.930	C3—C4—H9	121.37	120.7	C20—C23—H27	119.81	119.7
C11—H12	1.096	0.930	C5—C4—H9	120.32	120.7	C25—C23—H27	120.05	119.7
C11—N13	1.279	1.266	C4—C5—N6	123.50	123.64	C21—C25—C23	119.87	120.12
N13—N14	1.353	1.375	C4—C5—H10	120.49	118.2	C21—C25—H28	120.01	119.9
N14—H15	1.016	0.86	N6—C5—H10	116.00	118.2	C23—C25—H28	120.11	119.9
N14—C16	1.391	1.354	C1—N6—C5	117.88	117.44	Dihedral angle (°)	Cal.[a]	X-ray[b]
C16—O17	1.212	1.224	C1—C11—H12	115.40	119.3	N6—C1—C2—C3	−0.01	0.7
C16—C18	1.503	1.489	C1—C11—N13	121.42	121.34	C11—C1—C2—C3	179.94	−178.35
C18—C19	1.401	1.384	H12—C11—N13	123.17	119.3	C2—C1—N6—C5	0.04	−0.3
C18—C20	1.400	1.382	C11—N13—N14	117.41	116.43	C11—C1—N6—C5	−179.92	178.87
C19—C21	1.393	1.382	N13—N14—H15	119.25	120.4	C2—C1—C11—N13	−0.50	3.5
C19—H22	1.085	0.930	N13—N14—C16	121.08	119.21	C1—C2—C3—C4	−0.03	−0.05
C20—C23	1.391	1.381	H15—N14—C16	119.27	120.4	C2—C3—C4—C5	0.03	−0.01
C20—H24	1.083	0.930	N14—C16—O17	123.10	122.23	C3—C4—C5—N6	0.00	0.6
C21—C25	1.393	1.368	N14—C16—C18	114.11	116.26	C1—C11—N13—N14	−179.32	178.34
C21—H26	1.084	0.930	O17—C16—C18	122.79	121.48	C11—N13—N14—C16	−175.09	−176.58
C23—C25	1.395	1.359	C16—C18—C19	123.43	123.52	N13—N14—C16—O17	3.18	−2.2
C23—H27	1.084	0.930	C16—C18—C20	117.30	117.58	N13—N14—C16—C18	−177.60	176.05
C25—H28	1.084	0.930	C19—C18—C20	119.24	118.60	N14—C16—C18—C19	29.65	22.1

[a] Calculated bond parameters using B3LYP/6-311++G (d, p) level.
[b] Observed data by X-ray diffraction method.

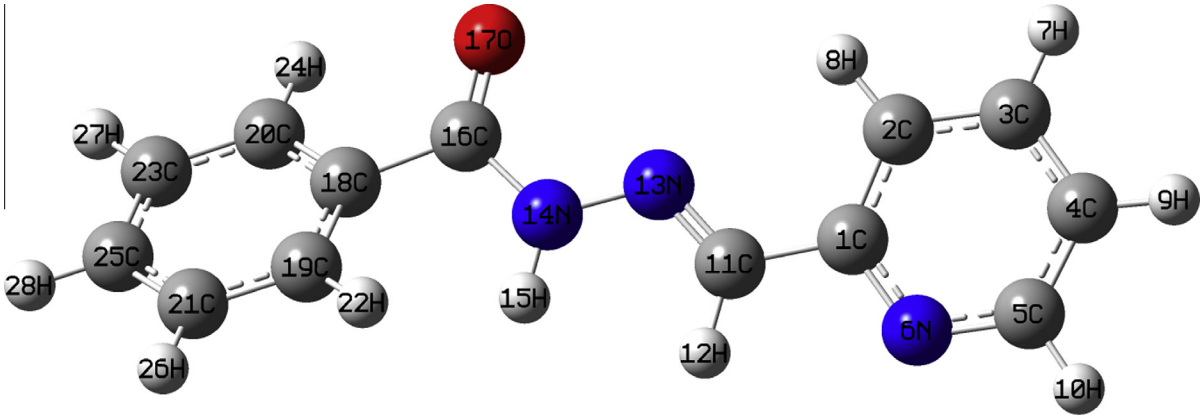

Fig. 1b. The optimized molecular structure of PMBH.

stretching vibration appears in the region of 3500–3220 cm^{-1} [28]. In the present investigation the stretching vibration of ν_{N-H} mode is recorded at 3349 cm^{-1} as a medium intensity band in FT-IR spectrum, whereas the calculated wavenumber assigned at 3369 cm^{-1} (mode no: 1) and its TED value is 100%. It is found that a small deviation between experimental and theoretical value is only because of the intra-molecular charge transfer between amino and carbonyl group in the hydrazone linkage.

The in-plane bending of δ_{N-H} ($\delta_{H15-N14-N13}$, $\delta_{H15-N14-C16}$: 30, 25%) was recorded as a mixed vibration of $\nu_{C16-N14}$ (12%) which shows as weak band at 1516 cm^{-1} (weak) in FT-IR whereas the calculated wavenumber lies at 1492 cm^{-1} (mode no: 18). The experimental frequency shows a positive deviation with the theoretical value. This assignment is visually verified by Gauss View program. The out-of-plane deformation of N—H was recorded at 567 (FT-IR: weak). This observed band is coinciding with the calculated value of 523 cm^{-1} (mode no. 60) for $\Gamma C_{18}—C_{16}—N_{14}—H_{15}$ (26%). The above recorded and calculated values were coinciding well with literature [29].

C—H vibrations

The existence of one or more aromatic rings in a structure is normally determined from the C—H and C=C—C ring related vibrations [30]. For phenyl ring in heteroaromatic structure, the C—H stretching vibrations normally occur in the region of 3100–3000 cm^{-1} [31]. In the present study, the ν_{C-H} stretching vibrations for phenyl ring observed at 3085 (w)/FT-IR, where as the calculated wavenumbers appeared in the region of 3075, 3066, 3056, 3046 and 3039 cm^{-1} (mode nos: 3, 5, 6, 8, 9). In the case of Pyridin ring, the stretching vibrations occur at 3061(m)

Table 3
The experimental and calculated frequencies of PMBH using B3LYP/6-311++G(d, p) level of basis set [harmonic frequency (cm^{-1}), IR (km/mol), Raman intensities, reduced masses (amu) and force constants (mdyn $Å^{-1}$)].

Modes	Frequencies (cm^{-1})				Intensity		Red. mass	Force const.	Vibrational Assignments[d] TED ⩾ 10%
	Unscaled	Scaled[a]	FT-IR	FT-Raman	IR[b]	Raman[c]			
1	3506	3369	3349sh		1.45	3.09	1.08	7.80	$\nu_{N14-H15(100)}$
2	3206	3080	3168m	3100w	0.67	0.91	1.10	6.63	$\nu_{C2-H8(92)}$
3	3201	3075	3085w		1.93	1.87	1.09	6.61	$\nu_{C20-H24(88)}$
4	3193	3068			4.49	2.82	1.10	6.58	$\nu_{C3-H7(15)}$, $\nu_{C4-H9(77)}$
5	3191	3066			3.88	2.51	1.10	6.58	$\nu_{C21-H26(36)}$, $\nu_{C23-H27(11)}$, $\nu_{C25-H28(41)}$
6	3181	3056			4.99	0.98	1.09	6.51	$\nu_{C19-H22(11)}$, $\nu_{C21-H26(35)}$, $\nu_{C23-H27(43)}$
7	3174	3050			2.10	1.12	1.09	6.46	$\nu_{C3-H7(77)}$, $\nu_{C4-H9(17)}$
8	3171	3046			0.92	1.15	1.09	6.44	$\nu_{C19-H22(24)}$, $\nu_{C23-H27(33)}$, $\nu_{C25-H28}$ (40)
9	3163	3039			1.55	0.35	1.09	6.40	$\nu_{C19-H22(60)}$, $\nu_{C21-H26(26)}$, $\nu_{C25-H28}$ (10)
10	3151	3027			7.11	1.70	1.09	6.37	$\nu_{C5-H10(95)}$
11	3049	2930	2922w		10.87	0.78	1.09	5.96	$\nu_{C11-H12(100)}$
12	1760	1691	1697vs	1683w	84.14	11.78	11.15	20.36	$\nu_{C16-O17(85)}$
13	1672	1606	1611ms	1627s	2.18	100.00	8.33	13.71	$\nu_{C11-N13(74)}$
14	1640	1576	1582ms	1580vs	1.80	16.28	5.50	8.72	$\nu_{C21-C19(21)}$ $\nu_{C23-C20(23)}$
15	1623	1560			8.51	85.28	5.28	8.19	$\nu_{C2-C1(10)}$, $\nu_{C3-C2(26)}$, $\nu_{C5-C4(12)}$, $\nu_{N6-C5(11)}$
16	1619	1556			1.80	1.60	5.51	8.51	$\nu_{C19-C18(16)}$ $\nu_{C20-C18(14)}$, $\nu_{C25-C21(19)}$, $\nu_{C25-C23(20)}$,
17	1606	1543		1532w	3.76	0.26	5.72	8.69	$\nu_{C2-C1(11)}$, $\nu_{C4-C3(31)}$, $\nu_{N6-C1(15)}$
18	1553	1492	1516w		100.00	15.69	1.85	2.63	$\nu_{C16-N14(12)}$, $\delta_{H15-N14-N13(30)}$, $\delta_{H15-N14-C16(25)}$
19	1521	1462		1454w	2.25	0.98	2.16	2.95	$\nu_{CC(26)}$, $\delta_{HCC(29)}$, $\delta_{CCH(28)}$
20	1496	1438	1430ms		35.96	7.71	2.14	2.82	$\nu_{N6-C1(14)}$, $\delta_{H10-C5-C4(14)}$, $\delta_{N6-C5-H10(16)}$
21	1476	1418		1422w	1.12	0.19	2.16	2.77	$\nu_{C21-C19(11)}$, $\nu_{C23-C20(10)}$, $\delta_{H28-C25-C21(13)}$, $\delta_{H28-C25-C23(13)}$
22	1463	1406	1361ms	1370ms	12.40	20.93	2.18	2.74	$\nu_{C2-C1(11)}$, $\delta_{C4-C3-H7(13)}$, $\delta_{H9-C4-C3(16)}$, $\delta_{C5-C4-H9(13)}$
23	1366	1313			5.73	1.27	1.59	1.74	$\delta_{H12-C11-C1(19)}$, $\delta_{H12-C11-N13(27)}$
24	1352	1299	1300ms	1300w	0.37	0.17	1.69	1.82	$\nu_{C21-C19(13)}$, $\nu_{C23-C20(13)}$, $\nu_{C25-C21(12)}$, $\nu_{C25-C23(10)}$
25	1333	1281			0.42	0.11	3.43	3.59	$\nu_{C19-C18(13)}$, $\nu_{C20-C18(12)}$
26	1318	1267	1266w	1261m	1.35	15.60	2.08	2.13	$\nu_{C2-C1(16)}$, $\nu_{N6-C1(15)}$, $\nu_{N6-C5(12)}$
27	1303	1252			0.02	4.60	2.84	2.84	$\nu_{N6=C5(32)}$, $\delta_{H8-C2-C1(13)}$, $\delta_{N6-C5-H10(15)}$
28	1260	1211		1228w	52.70	0.37	2.46	2.30	$\nu_{N6-C1(10)}$, $\nu_{C18-C16(10)}$, $\delta_{H12-C11-N13(10)}$
29	1249	1200			78.72	77.21	2.85	2.62	$\nu_{C18-C16(22)}$
30	1203	1156	1175	1165ms	11.18	4.37	1.15	0.98	$\nu_{C21-C19(11)}$, $\delta_{C21-C19-H22(11)}$, $\delta_{H26-C21-C19(13)}$, $\delta_{C25-C21-H26(13)}$
31	1184	1138			0.07	0.54	1.12	0.92	$\delta_{H27-C23-C20(12)}$, $\delta_{C25-C23-H27(12)}$, $\delta_{H28-C25-C21(19)}$, $\delta_{H28-C25-C23(19)}$
32	1173	1127			7.59	8.25	1.15	0.94	$\nu_{N14-N13(52)}$
33	1170	1124	1012w	1103w	81.23	35.00	3.80	3.07	$\delta_{H7-C3-C2(18)}$, $\delta_{C4-C3-H7(17)}$, $\delta_{H9-C4-C3(10)}$, $\delta_{C5-C4-H9(12)}$
34	1115	1071	1092m		0.55	1.66	1.65	1.21	$\nu_{C5-C4(11)}$, $\delta_{C3-C2-H8(11)}$, $\delta_{H9-C4-C3(12)}$
35	1107	1063			6.96	3.61	1.67	1.20	$\nu_{C21-C19(14)}$
36	1076	1034		1043w	2.83	0.33	3.21	2.19	$\nu_{N14-N13(12)}$, $\nu_{C16-N14(25)}$
37	1064	1022			1.29	2.81	2.20	1.47	$\nu_{C4-C3(31)}$, $\nu_{C5-C4(23)}$
38	1047	1006		1004ms	3.77	1.75	2.48	1.60	$\nu_{C25-C21(21)}$, $\nu_{C25-C23(27)}$
39	1017	977			0.07	0.07	1.32	0.80	$\nu_{CC(38)}$, $\delta_{CCC(46)}$
40	1016	976			0.91	8.85	5.74	3.49	$\Gamma_{H7-C3-C2-H8(34)}$, $\Gamma_{H9-C4-C3-H7(24)}$
41	1011	972			0.16	0.13	1.33	0.80	$\Gamma_{H27-C23-C20-H24(23)}$, $\Gamma_{H28-C25-C21-H26(14)}$, $\Gamma_{H28-C25-C23-H27(24)}$
42	1009	970			2.39	17.38	7.25	4.35	$\nu_{N6-C1(12)}$, $\nu_{N6-C5(10)}$
43	993	954			0.43	0.14	1.37	0.80	$\Gamma_{H10-C5-C4-C3(12)}$, $\Gamma_{C1-N6-C5-H10(14)}$, $\Gamma_{H10-C5-C4-H9(34)}$
44	984	946	941w		0.83	0.01	1.43	0.82	$\Gamma_{H26-C21-C19-H22(19)}$, $\Gamma_{H27-C23-C20-H24(16)}$, $\Gamma_{H28-C25-C21-H26(17)}$
45	960	922			4.32	1.06	1.53	0.83	$\Gamma_{H12-C11-C1-C2(13)}$, $\Gamma_{H12-C11-C1-N6(19)}$, $\Gamma_{N14-N13-C11-H12(39)}$
46	944	907	914w	911w	0.72	0.24	1.48	0.78	$\Gamma_{H26-C21-C19-H22(16)}$, $\Gamma_{H28-C25-C23-H27(11)}$
47	936	900			8.70	2.55	4.53	2.34	$\delta_{O17-C16-N14(11)}$
48	916	880	869w	868w	0.02	0.06	1.31	0.65	$\Gamma_{C4-C3-C2-H8(15)}$, $\Gamma_{H9-C4-C3-H7(20)}$, $\Gamma_{H8-C2-C1-C11(13)}$
49	860	826			0.79	0.15	1.29	0.56	$\Gamma_{HCCC(59)}$, $\Gamma_{CCCH(32)}$
50	856	822			1.47	2.95	4.61	1.99	$\nu_{C2-C1(16)}$, $\nu_{C11-C1(13)}$
51	806	774			2.36	1.60	2.78	1.06	$\Gamma_{C20-C18-C16-O17(12)}$
52	793	762	765ms	769w	9.01	0.12	1.85	0.69	$\Gamma_{H7-C3-C2-C1(13)}$
53	757	727			4.89	0.01	2.05	0.69	$\Gamma_{H8-C2-C1-N6(11)}$, $\Gamma_{H9-C4-C3-C2(10)}$, $\Gamma_{N6=C5-C4-H9(14)}$
54	720	691			18.74	0.32	1.78	0.54	$\Gamma_{HCCC(37)}$, $\Gamma_{CCCH(21)}$
55	704	676			3.00	0.13	2.89	0.84	$\Gamma_{CCCC(45)}$
56	695	668			8.36	0.35	6.49	1.85	$\delta_{C21-C25-C23(14)}$
57	679	652			1.09	1.91	5.81	1.58	$\delta_{CCC(21)}$, $\delta_{NCC(22)}$, $\delta_{CCH(11)}$
58	633	608	623ms	620w	1.32	1.06	6.97	1.64	$\delta_{C21-C19-C18(13)}$, $\delta_{C23-C20-C18(14)}$, $\delta_{C25-C21-C19(15)}$, $\delta_{C25-C23-C20(15)}$
59	632	607			0.84	1.81	6.52	1.54	$\delta_{C4-C3-C2(19)}$, $\delta_{C1-N6-C5(20)}$
60	544	523	567w		18.49	3.43	1.38	0.24	$\Gamma_{H15-N14-N13-C11(41)}$, $\Gamma_{O17-C16-N14-H15(19)}$, $\Gamma_{C18-C16=N14-H15(26)}$
61	532	511	512w	516w	1.23	0.39	3.54	0.59	$\Gamma_{N6=C5-C4-C3(12)}$
62	524	503			0.92	0.33	2.83	0.46	$\delta_{O17-C16-C18(16)}$
63	488	469	459w		0.26	0.51	5.81	0.82	$\delta_{N6-C1-C11(13)}$
64	420	403			2.38	0.42	4.34	0.45	$\Gamma_{CCCC(31)}$
65	417	401			1.56	0.20	3.67	0.38	$\Gamma_{C4-C3-C2-C1(19)}$, $\Gamma_{C5-C4-C3-C2(10)}$, $\Gamma_{C1-N6-C5-C4(16)}$
66	414	398			0.03	0.24	2.96	0.30	$\Gamma_{C25-C21-C19-C18(17)}$, $\Gamma_{C25-C23-C20-C18(17)}$
67	379	364			0.07	0.13	8.08	0.68	$_{C18-C16(19)}$, $\delta_{N14-N13-C11(11)}$, $\delta_{O17-C16-N14(15)}$
68	320	307		328m	0.79	0.61	5.60	0.34	$\Gamma_{N14-N13-C11-C1(26)}$
69	261	251		261m	0.99	1.38	4.97	0.20	$\delta_{C19-C18-C16(12)}$, $\delta_{C20-C18-C16(14)}$
70	243	234			0.58	1.29	6.63	0.23	$\nu_{C16-N14(10)}$, $\delta_{N6-C1-C11(11)}$, $\delta_{C16-N14-N13(11)}$

Table 3 (*continued*)

Modes	Frequencies (cm^{-1})				Intensity		Red. mass	Force const.	Vibrational Assignments[d] TED ⩾ 10%
	Unscaled	Scaled[a]	FT-IR	FT-Raman	IR[b]	Raman[c]			
71	230	221			4.44	1.95	3.19	0.10	$\delta_{CCC(11),\ HCCC(11)}$
72	178	171		172w	1.74	2.25	5.12	0.10	$\Gamma_{C16-N14-N13-C11(10)}$, $\Gamma_{C23-C20-C18-C16(10)}$
73	125	120			0.68	2.54	6.01	0.06	$\Gamma_{C16-N14-N13-C11(16)}$, $\Gamma_{C19-C18-C16-O17(11)}$
74	120	115		119ms	1.89	1.81	5.47	0.05	$\delta_{N13-C11-C1(12)}$, $\delta_{C18-C16-N14(14)}$
75	64	62		69ms	0.89	9.91	5.39	0.01	$\Gamma_{N13-C11-C1-N6(14)}$, $\Gamma_{CCCN(28)}$, $\Gamma_{CCCO(24)}$
76	47	45			0.76	5.36	5.68	0.01	$\delta_{N13-C11-C1(11)}$, $\delta_{N14-N13-C11(21)}$, $\delta_{C16-N14-N13(16)}$
77	33	32			0.27	21.04	4.07	0.00	$\Gamma_{N13-C11-C1-N6(10)}$, $\Gamma_{C16-N14-N13-C11(20)}$, $\Gamma_{CCCN(23)}$
78	32	31			0.48	6.02	5.67	0.00	$\Gamma_{N14-N13-C11-C1(14)}$, $\Gamma_{O17-C16-N14-N13(16)}$, $\Gamma_{C18-C16-N14-N13(33)}$

ν: Stretching, δ: in-plane-bending, Γ: out-of-plane bending, vw: very week, w:week, m: medium, s: strong, vs: very strong.

[a] Scaling factor: 0.9608.

[b] Relative IR absorption intensities normalized with highest peak absorption equal to 100.

[c] Relative Raman intensities calculated by Eq. (1) and normalized to 100.

[d] Total energy distribution calculated at B3LYP/6-311++G(d, p) level.

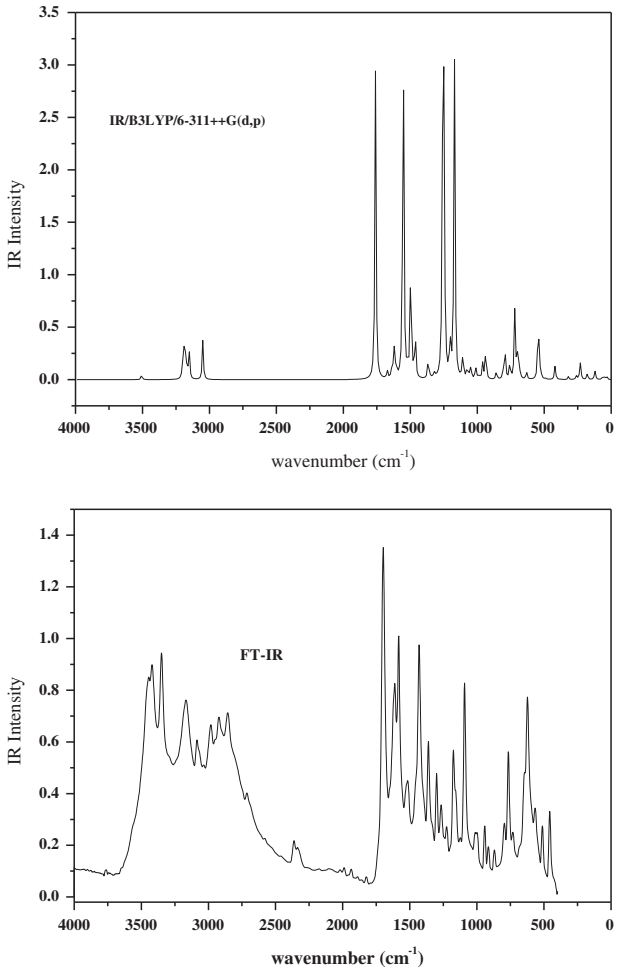

Fig. 2. The combined IR spectrum of PMBH.

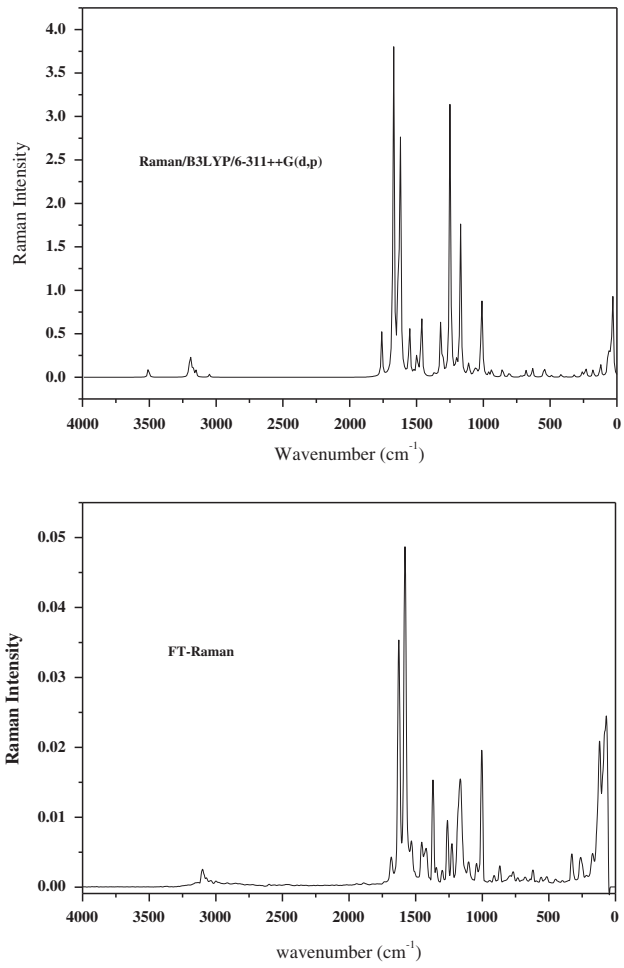

Fig. 3. The combined Raman spectra of PMBH.

cm^{-1}/FT-IR, 3100 cm^{-1}(w)/FT-Raman, where as the calculated wavenumbers appeared in the region of 3080, 3068, 3050 and 3027 cm^{-1} (mode nos: 2, 4, 7, 10). These assignments are in good agreement with literature values [31] and also well supported by the TED values.

In aromatic compounds, the presence of C—H in-plane bending lies in the range of 1000–1300 cm^{-1} and the out-of-plane bending vibrations occur in the range of 750–1000 cm^{-1} [29,32]. In our present study, the C—H in-plane bending vibration for phenyl ring appeared at 1175 cm^{-1} in FT-IR and 1422 (w) and 1165 (ms) cm^{-1} in FT-Raman where as the calculated values lies at 1418, 1156, 1138 (mode nos: 21, 30, 31). For pyridin ring, the C—H in-plane bending vibrations occur at 1430(ms), 1361 (ms), 1012 (w), 1092 (m) in FT-IR and 1454 (w), 1370 (ms), 1103 (w) in FT-Raman, where as the calculated values lies at 1462, 1438, 1406, 1252, 1124, 1071 (mode nos: 19, 20, 22, 27, 33, 34).

The out-of-plane bending vibration of Γ_{CCCH} in phenyl ring lies at 941(w), 914(w) cm^{-1} in FT-IR and 911(w) in FT-Raman, whereas the calculated wavenumbers shown as 972, 946, 907 (mode nos:

41, 44, 46). Likewise for the pyridin ring, the Γ_{CCCH} appears at 869 (w), 765 (ms) cm^{-1} in FT-IR and the corresponding Raman counterpart shown at 868 (w), 769 (w), whereas the calculated value lies in the range of 976, 954, 880, 762, 727 cm^{-1} (mode nos: 40, 43, 48, 52, 53). These assignments are will supported by literature value [29,32] and also find support from TED values.

Further, the mode numbers 11, 23 and 45 were assigned to $\nu_{C11-H12}$, $\delta_{C11-H12}$ and $\Gamma_{C11-H12}$ respectively and the experimental value of FT-IR in mode no 11 assigned at 2922 cm^{-1} with 100% TED value.

C=O vibrations

The multiple bonded group is highly polar >(C=O)< and therefore it gives rise to an intense infrared absorption band. The carbon–oxygen double bond is formed by Pπ–Pπ bonding between carbon and oxygen. The lone pair of electron in oxygen also determines the nature of the carbonyl group [33]. The carbonyl C=O stretching vibration is expected to occur in the region 1680–1715 cm^{-1} [34,35]. In our present study the carbonyl group stretching vibration occurs at 1697 cm^{-1} as strong band in FT-IR spectrum and weak FT-Raman band at 1683 cm^{-1}. For the same mode the harmonic frequency 1691 cm^{-1} (mode no: 12) is having 85% of TED value. The carbonyl group (C_{16}=O_{17}) assigned in the present study is in line with calculated and also with literature values [34,35].

The calculated frequency of C_{16}=O_{17} in-plane bending vibration lies at 900 cm^{-1} (mode no: 47) with low percentage value (11%) of TED. The out-of-plane bending of $\Gamma_{C=O}$ was recorded at 567 cm^{-1}/FT-IR as a weak band whereas the corresponding calculated value lies at 523 (mode no: 60) as a mixed vibration with $\Gamma_{N14-H15}$ (16% TED). The above in-plane and out-of-plane deformations of C=O group is well supported by the literature value [36].

C=N, C–N and N–N vibrations

The hydrazone linkage fuses the phenyl and pyridin rings, which leads the vibrations such as C=N, C–N and N–N stretching as well as bending modes. The C=N stretching vibration appears in the region of 1670–1600 cm^{-1} [37]. Subashchandrabose et al. [38] assigned the C=N stretching vibration at 1639 cm^{-1}. The same mode was recorded at 1616/1618 cm^{-1} (FT-IR/FT-Raman) in our previous study [39]. In the present study the C_{11}=N_{13} stretching vibration in hydrazone linkage appeared at 1611 cm^{-1} as a medium strong band in FT-IR and 1627 cm^{-1} as a strong band in FT-Raman spectra. Their corresponding theoretical wavenumber was calculated at 1606 cm^{-1} (mode no: 13). The recorded and calculated frequencies were supported by the literature [38,39]. In pyridin ring, the $\nu_{C5=N6}$ band assigned at 1560 cm^{-1} (mode no: 15).

Silverstein et al. [31] assigned C–N stretching absorption in the region 1382–1266 cm^{-1} for aromatic amines. The C_{16}–N_{14} stretching vibration appears at 1516 cm^{-1} as a mixed vibration of $\delta_{H15N14N13\ (30\%)}$ and $\delta_{H15N14C25\ (25\%)}$, which correlates well with computed value 1492 cm^{-1} (mode no: 18). In pyridin ring, the ν_{C1-N6} mode assigned to 1266 (FT-IR: weak)/1261 cm^{-1} (FT-Raman: medium) and its corresponding computed wavenumber is 1267 cm^{-1} (mode no: 26). These observed and calculated frequencies of ν_{C-N} coincide well with the literature. The bond N_{14}–N_{13} in hydrazone linkage fuses the two rings. The stretching, in-plane bending and out-of-plane bending vibrations of (N_{14}–N_{13}) were assigned to mode nos: 32, 67 and 68 respectively. The mode no 68 is coinciding with observed FT-Raman spectrum (328 cm^{-1}).

In hydrazone link, the in-plane bending vibration of $\delta_{C11=N13}$ and $\delta_{C16-N14}$ were assigned to 1313 (mode no: 23) and 1034 cm^{-1} (mode no: 36) respectively while their corresponding out-of-plane modes were assigned to mode numbers 45 (922 cm^{-1}) and 60 (523 cm^{-1}) respectively. These assignments find support from observed bands (1043 cm^{-1}/FT-Raman, 567 cm^{-1}/FT-IR). The mode numbers 27, 63 and 53, 65 are belongs to $\delta_{C5=N6}$, δ_{C1-N6} and $\Gamma_{C5=N6}$, Γ_{C1-N6} modes of pyridin ring respectively. These assignments were in line with observed spectral value (459 cm^{-1}/FT-IR). The literature survey reveals that the δ_{CN} and Γ_{CN} vibrations are assigned in the range of 1078–440 cm^{-1} and 671–235 cm^{-1} respectively by Krishnakumar and Muthunatesan [40] in the case of 2,4-dihyroxy-3-nitropyridin.

C=C, C–C vibrations

The phenyl ring carbon–carbon (C–C) stretching vibrations are reported in the regions of 1625–1590, 1590–1575, 1540–1470, 1465–1430 and 1380–1280 cm^{-1} by Varsanyi [32]. Krishnakumar and Muthunatesan [40] assigned C–C stretching absorption in the region of 1668–1218 cm^{-1} for some substituted pyridins. The medium bands observed at 1532 (weak), 1370, 1261 cm^{-1} in Raman spectrum and 1361, 1266 cm^{-1} (weak) in FT-IR spectrum correspond to $\nu_{(C-C)}$ vibrations of pyridine ring. Similarly the observed bands 1582/1580, 1300/1300 (FT-IR/FT-Raman) and 1422 cm^{-1} (FT-Raman) were attributed to $\nu_{(C-C)}$ modes of phenyl ring. The harmonic frequencies in the ranges of 1560–1267 cm^{-1} (mode nos: 15, 17, 22, 26) and 1576–1281 cm^{-1} (mode nos: 14, 16, 21, 24, 25) were belong to $\nu_{(C-C)}$ modes of pyridin and benzene rings respectively. These assignments coinciding well with the literature value [41]. The calculated frequencies 1200 mode no: 29 and 822 cm^{-1}/mode no: 50 are attributed to $\nu_{C18-C16}$ and $\nu_{(C11-C1)}$ modes respectively.

The C–C–C in-plane and out-of-plane bending modes are the modes associated with smaller force constant than the stretching one and hence assigned to lower frequencies. The ring trigonal bending modes were calculated respectively at 668, 608 and 977 cm^{-1} for phenyl ring, whereas the Γ_{CCC} mode assigned to 403 (mode no: 64) and 398 cm^{-1} (mode no: 66). The observed FT-IR/623 cm^{-1} and Raman/620 cm^{-1} bands support the δCCC mode with considerable TED values. In pyridin ring, the in-plane and the out-of-plane deformations appeared at 607 and 401 cm^{-1} (mode nos: 59 and 65) as mixed vibrations of the in-plane and the out-of-plane modes of C_1–N_6. These assignments find support from literatures for phenyl [42] and Pyridin rings [40].

Prediction of hyperpolarizability

The first order hyperpolarizabilities of PMBH was calculated using B3LYP/6-311++G (d, p) level of basis set, based on the finite-field approach. In the presence of an applied electric field, the energy of a system is a function of the electric field. The first order hyperpolarizability is a third rank tensor that can be described by a $3 \times 3 \times 3$ matrix. The 27 components of the 3D matrix can be reduced to 10 components due to Kleinman symmetry [43]. It can be given in the lower tetrahedral format. It is obvious that the lower part of the $3 \times 3 \times 3$ matrices is a tetrahedral. The components of β are defined as the coefficients in the Taylor series expansion of the energy in the external electric field. When the external electric field is weak and homogeneous, this expansion becomes:

$$E = E^0 - \mu_\alpha F_\alpha - 1/2\alpha_{\alpha\beta}F_\alpha F_\beta - 1/6\beta_{\alpha\beta\gamma}F_\alpha F_\beta F_\gamma \quad (2)$$

where E^0 is the energy of the unperturbed molecules, F_α is the field at the origin, and μ_α, $\alpha_{\alpha\beta}$, $\beta_{\alpha\beta\gamma}$ is the components of the dipole moment, polarizability and the first order hyperpolarizabilities respectively. The total static dipole moment μ, the mean polarizability α_0, the anisotropy of polarizability $\Delta\alpha$ and the mean first order hyperpolarizability β_0, using the x, y, z components are defined as

$$\mu = \left(\mu_x^2 + \mu_y^2 + \mu_z^2\right)^{1/2} \quad (3)$$

Table 4
The second order perturbation theory analysis of Fock Matrix in NBO basis for PMBH.

Type	Donor (i)	ED/e	Acceptor (j)	ED/e	$E^{(2)}$ (kJ/mol)	E(j)–E(i) a.u	$F(i, j)$ a.u
π–π*	C1—N6	1.699	C2—C3	0.277	52.80	0.33	0.06
			C4—C5	0.301	110.54	0.32	0.08
			C11—N13	0.174	53.76	0.31	0.06
π–π*	C2—C3	1.649	C1—N6	0.433	112.42	0.27	0.08
			C4—C5	0.301	75.19	0.28	0.06
π–π*	C4—C5	1.635	C1—N6	0.433	71.21	0.27	0.06
			C2—C3	0.277	87.07	0.29	0.07
π–π*	C11—N13	1.922	C1—N6	0.433	43.05	0.34	0.06
			C11—N13	0.174	4.06	0.35	0.02
π–π*	C16—O17	1.981	C16—O17	0.266	2.80	0.42	0.02
			C18—C19	0.373	14.64	0.41	0.04
π–π*	C18—C19	1.659	N14—C16	0.087	2.93	0.68	0.02
			C16—O17	0.266	64.27	0.3	0.06
			C20—C23	0.295	80.63	0.29	0.07
			C21—C25	0.323	80.12	0.29	0.07
π–π*	C20—C23	1.647	C18—C19	0.373	85.44	0.28	0.07
			C21—C25	0.323	89.29	0.28	0.07
π–π*	C21—C25	1.652	C18—C19	0.373	88.99	0.28	0.07
			C20—C23	0.295	77.24	0.29	0.07
π–π*	O17	1.857	N14—C16	0.087	120.29	0.66	0.13
			C16—C18	0.068	78.66	0.66	0.10
π–π*	C1—N6	0.433	C2—C3	0.277	645.38	0.02	0.09
			C4—C5	0.301	765.80	0.02	0.08
π–π*	C11—N13	0.174	C2—C3	0.277	3.05	0.02	0.01
π–π*	C16—O17		C16—O17	0.017	12.01	0.56	0.10
π–π*	C18—C19		N14—C16	0.087	2.51	0.39	0.03
			C16—O17	0.266	566.68	0.01	0.07

[a] $E^{(2)}$ means energy of hyper conjugative interaction (stabilization energy).
[b] Energy difference between donor (i) and acceptor (j) nbo orbitals.
[c] F(i, j) is the Fock matrix element between i and j nbo orbitals.

$$\alpha_0 = \frac{\alpha_{xx} + \alpha_{yy} + \alpha_{zz}}{3} \tag{4}$$

$$\Delta\alpha = 2^{-1/2}\left[(\alpha_{xx} - \alpha_{yy})^2 + (\alpha_{yy} - \alpha_{zz})^2 + (\alpha_{zz} - \alpha_{xx})^2 + 6\left(\alpha_{xy}^2 + \alpha_{yz}^2 + \alpha_{xz}^2\right)\right]^{1/2} \tag{5}$$

$$\beta_0 = \left(\beta_x^2 + \beta_y^2 + \beta_z^2\right)^{1/2} \tag{6}$$

Many organic molecules, containing conjugated π electrons were characterized by large values of molecular first order hyper polarizabilities and analyzed by means of vibrational spectroscopy [44–47]. The intra-molecular charge transfer from the donor to acceptor group through a single–double bond conjugated path can induce large variations on both the molecular dipole moment and the molecular polarizability [48].

In this study the total molecular dipole moment (μ) and mean first order hyperpolarizability (β_0) were calculated as 1.025 Debye and 4.360×10^{-30} esu respectively. The total dipole moment of the title compound is approximately higher and the first order hyperpolarizability (β_0) of the title molecule is twelve times greater than that of urea. This molecule has considerable NLO activity and the hyperpolarizabilities of PMBH were given in Table S1 (Supplementary material).

Natural bond orbital (NBO) analysis

The hyperconjugation gives as stabilizing effect that arises from an overlap between an occupied orbital with another neighboring electron deficient orbital, when these orbitals are properly oriented. This non-covalent bonding (antibonding) interaction can be quantitatively described in terms of the NBO analysis, which is expressed by means of the second-order perturbation interaction energy ($E^{(2)}$) [49–52]. This energy represents the estimate of the off-diagonal NBO Fock matrix elements. It can be deduced from the second-order perturbation approach [53]

$$E^{(2)} = \Delta E_{ij} = q_i \frac{F(i,j)^2}{\varepsilon_j - \varepsilon_i} \tag{7}$$

Table 5
The excitation energies and oscillator strengths of PMBH.

Excited State1	Singlet-A	Excitation energy		Observed energy	Oscillator strength
59 → 60	0.64053	4.1045 eV	302.07 nm	301 nm	f = 0.8163
Excited State 2	Singlet-A	4.1942 eV	295.61 nm		f = 0.0334
55 → 60	0.26360				
57 → 60	−0.19461				
58 → 60	0.57646				
58 → 61	−0.11093				
Excited State 3	Singlet-A	4.3053 eV	287.98 nm		f = 0.0022
55 → 60	0.19178				
57 → 60	0.63149				
57 → 61	0.17116				
58 → 60	0.11460				

where q_i is the donor orbital occupancy, ε_i and ε_j are diagonal elements (orbital energies) and $F(i, j)$ is the off diagonal NBO Fock matrix elements. NBO analysis of PMBH has been performed, in order to explain the intra-molecular charge transfer within the molecule. The intra-molecular hyperconjugative interaction is due to the overlap between π(C—C) and π*(C—C) the orbitals, which results in intra-molecular charge transfer, appeared in the molecular system [48].

In the present study, the NBO analysis mainly focused on the π–π* interactions. In the same way, the interaction between $\pi C_1—N_6$ and $\pi^* C_2—C_3$, $C_4—C_5$, $C_{11}—N_{13}$ are reveals the hyperconjugative energy about 52.80, 110.54, 53.76 kJ/mol respectively. It could be analyzed that the strong delocalization occurs in pyridin, it is mainly due to the presence of C=N—C. This bond also affects the vibrational frequencies of C—C bond in pyridin ring. Similarly the conjugative π bonds in the phenyl ring shows maximum delocalization during the interaction with π* acceptor bonds. It is evident from our title compound that the $\pi C_{18}—C_{19}$, $C_{20}—C_{23}$ and $C_{21}—C_{25}$ delocalize more energy to the acceptor bond (π* acceptor). The electron density of donor bonds decreases while the acceptor (π*) bond electron density increases. From the Table 4, the π*C1—N6 delocalizes the maximum energy 645.88 and 765.80 kJ/mol to $\pi C_2—C_3$ and $C_4—C_5$ bond respectively. Similarly, the $\pi^* C_{18}—C_{19}$ bond transfers the energy about 566.68 kJ/mol to $C_{16}—O_{17}$ bond. The NBO analysis also predicts the interaction between lone pair and acceptor bonds within the molecule.

Band gap energy analysis

The ultraviolet visible (UV–Visible) spectrum reveals that the promotion of an electron in an occupied molecular orbital (MO) of ground electronic state molecule into a virtual MO, thus forming an electronically excited state [54]. The UV analysis was carried out using B3LYP/6-311++G (d, p) level of basis set for PMBH. The highest occupied molecular orbital (HOMO) and lowest unoccupied molecular orbital (LUMO) are the main orbitals that take part in chemical stability. The HOMO represents the ability to donate an electron and LUMO represents the ability to obtain an electron. This also predicted that the nature of electrophiles and nucleophiles to the atom where the HOMO and the LUMO are stronger.

The UV–Visible spectrum recorded for PMBH molecule shows the transition at 301 nm. Its corresponding theoretical prediction reveals three excited states namely excited state 1, 2 and 3(ES_1, ES_2 and ES_3). The predicted ES_1 exactly matches with the observed value of 301 nm, the ES_2 lies at 295.61 nm and the ES_3 lies at 287.98 nm. The band gap energy of PMBH was calculated about 4.691 eV using TD-B3LYP/6-311++G (d, p) level. The recorded and calculated energies of frontier molecular orbitals were listed in Table 5. The recorded UV–Visible spectrum and frontier molecular orbitals were shown in Figs. 4 and 5 respectively.

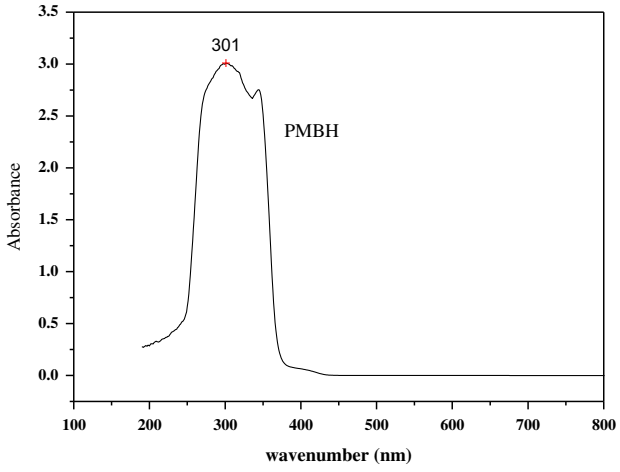

Fig. 4. The recorded UV visible spectrum of PMBH.

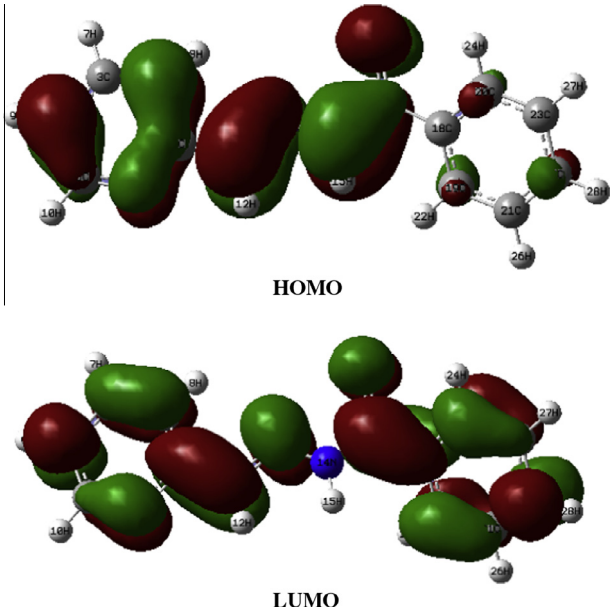

Fig. 5. The frontier molecular orbitals of PMBH.

Electrostatic potential

The information provided by inspection of the HOMO and the LUMO is thus visualizing the electrostatic potential (ESP). The electrophiles tend to negative ESP and the nucleophiles tend to region of positive ESP. In accordance with this the carbonyl and pyridin ring behaves as electrophiles region and it is denoted as red color. The molecular electrostatic potential was calculated with B3LYP/6-311++G (d, p) level of theory. The calculated electrostatic energy for carbonyl group is about −22.40 a.u (−609.540 eV). Similarly, the nucleophiles region was graphically shown as blue color. It is possibly denoted by blue color and expressed as electron deficiency in those regions, which also denotes nucleonic energy of the LUMO orbitals. The calculated electrostatic potential energy are about −18.32 a.u (N_{14}: −498.517 eV) and −18.35 a.u (N_{13}: -499.333) for the hydrazone region. The ESP diagram is shown in Fig. 6.

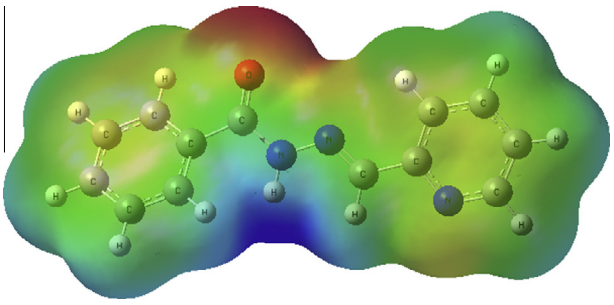

Fig. 6. The electrostatic potential (ESP) diagram of PMBH.

Conclusion

In the present study the PMBH molecule was synthesized and it was characterized by X-ray diffraction, FT-IR, FT-Raman and UV–Visible spectra. The observed geometrical parameters of PMBH molecule were coinciding well with the calculated parameters. The recorded vibrational spectra (FT-IR, FT-Raman) of PMBH shows the bands within the characteristic region and the same bands were reproduced by the theoretical calculation. The vibrational band assignments were carried out by the TED analysis. The result obtained from the TED analysis clearly explains the vibration of all functional groups. The hyperpolarizability of the PMBH molecule was studied and found to be higher value while comparing with similar molecules. The charge delocalization within the molecule was calculated in which the π–π^* excitation were transferred more hyperconjugative energy. The observed and predicted UV–Visible spectra were showed the excitation at 301 and 207 nm respectively. The band gap energy was determined about 4.691 eV. The MEP analysis exploits the reactive path of the molecule.

Appendix A. Supplementary material

Supplementary data associated with this article can be found, in the online version, at http://dx.doi.org/10.1016/j.molstruc.2014.04.060.

References

[1] N.P. Belskaya, W. Dehaen, V.A. Bakulev, Arkivoc (i) (2010) 275–332.
[2] S. Kim, J.Y. Yoon, Sci. Synth. 27 (2004) 671–722.
[3] R. Brehme, D. Enders, R. Fernandez, J.M. Lassaletta, Eur. J. Org. Chem. 34 (2007) 5629–5660.
[4] S. Dadiboyena, A. Nefzi, Eur. J. Med. Chem. 46 (2011) 5258–5275.
[5] Y.P. Kitaev, B.I. Buzykin, T.V. Troepol'skaya, Russ. Chem. Rev. 39 (1970) 441–456.
[6] A.M. Wu, P.D. Senter, Nat. Biotechnol. 23 (2005) 1137–1146.
[7] R.W. Binkley, Tetahedron Lett. 23 (1969) 1893–1896.
[8] S.D. Carson, J. Org. Chem. 35 (1970) 2734–2736.
[9] R.P. Bhole, K.P. Bhusari, QSAR Comb. Sci. 28 (2009) 1405–1417.
[10] C. Loncle, J.M. Brunel, N. Vidal, M. Dherbomez, Y. Letourneux, Eur. J. Med. Chem. 39 (2004) 1067–1071.
[11] K.K. Bedia, O. Elcin, U. Seda, K. Fatma, S. Nathaly, R. Sevim, A. Dimoglo, Eur. J. Med. Chem. 41 (2006) 1253–1261.
[12] K.K.V. Raj, B. Narayana, B.V. Ashalatha, N.S. Kumari, B.K. Sarojini, Eur. J. Med. Chem. 42 (2007) 425–429.
[13] G.M. Sheldrick, Acta Cryst. D65 (2009) 112–122.
[14] Bruker, APEX2 and SAINT. Bruker AXS Inc., Madison, Wisconsin, USA, 2008.; Bruker, Med. Chem. 39 (2004) 1067–1071.
[15] A.L. Spek, Acta Cryst. D65 (2009) 148–155.
[16] M.J. Frisch, G.W. Trucks, H.B. Schlegel, G.E. Scuseria, M.A. Robb, J.R. Cheeseman, J.A. Montgomery Jr., T. Vreven, K.N. Kudin, J.C. Burant, J.M. Millam, S.S. Iyengar, J. Tomasi, V. Barone, B. Mennucci, M. Cossi, G. Scalmani, N. Rega, G.A. Petersson, H. Nakatsuji, M. Hada, M. Ehara, K. Toyota, R. Fukuda, J. Hasegawa, M. Ishida, T. Nakajima, Y. Honda, O. Kitao, H. Nakai, M. Klene, X. Li, Knox, H.P. Hratchian, J.B. Cross, C. Adamo, J. Jaramillo, R. Gomperts, R.E. Stratmann, O. Yazyev, A.J. Austin, R. Cammi, C. Pomelli, J.W. Ochterski, P.Y. Ayala, K. Morokuma, G.A. Voth, P. Salvador, J.J. Dannenberg, V.G. Zakrzewski, S. Dapprich, A.D. Daniels, M.C. Strain, O. Farkas, D.K. Malick, A.D. Rabuck, K. Raghavachari, J.B. Foresman, J.V. Ortiz, Q. Cui, A.G. Baboul, S. Clifford, J. Cioslowski, B.B. Stefanov, G. Liu, A. Liashenko, P. Piskorz, I. Komaromi, R.L. Martin, D.J. Fox, T. Keith, M.A. Al-Laham, C.Y. Peng, A. Nanayakkara, M. Challacombe, P.M.W. Gill, B. Johnson, W. Chen, M.W. Wong, C. Gonzalez, J.A. Pople, Gaussian 03, Revision C.02, Gaussian Inc, Wallingford, CT, 2004.
[17] H.B. Schlegel, J. Comput. Chem. 3 (1982) 214–218.
[18] G. Rauhut, P. Pulay, J. Phys. Chem. 99 (1995) 3093–3100.
[19] D. Michalska, Raint Program, Wroclaw University of Technology, Poland, 2003.
[20] D. Michalska, R. Wysokinski, Chem. Phys. Lett. 403 (2005) 211–217.
[21] R. Bikas, F. Sattarri, B. Notash, Acta Cryst. E68 (2012) m132–m133.
[22] H.H. Rassem, A. Salhin, B.B. Salleh, M.M. Rosti, H.K. Fun, Acta Cryst. E68 (2012) o1832.
[23] H. Kargar, R. Kia, M.N. Tahir, Acta Cryst. E68 (2012) o2321–o2322.
[24] J.X. Gou, M.Z. Song, C.G. Fan, Z.N. Yang, Acta Cryst. E65 (2009) o3207.
[25] Y. Nair, M. Sithambaresan, M.R. Prathapachandra Kurup, Acta Cryst. E68 (2012) o2709.
[26] C.B. Tang, Acta Cryst. E67 (2011) o271.
[27] L.J. Bellamy, The Infrared Spectra of Complex Molecules, vol. 2, Chapman and Hall, London, 1980.
[28] S. Gunasekaran, S.R. Varadhan, K. Manoharan, Asian J. Phys. 2 (1993) 165.
[29] G. Socrates, Infrared and Raman characteristic Group Frequencies Table and Charts, third ed., Wiley, Chichester, 2001.
[30] E. Fereyduni, E. Vessally, E. Yaaghubi, N. Sundaraganesan, Spectrochim. Acta A 81 (2011) 64–71.
[31] M. Silverstein, C.G. Basseler, C. Morill, Spectrometric Identification of Organic Compounds, Wiley, New York, 1981.
[32] G. Varsanyi, Assignments of vibrational spectra of 700 Benzene Derivatives, Wiley, New York, 1974.
[33] D.N. Sathyanarayanan, Vibrational spectroscopy theory and applications, New Age International Publishers, New Delhi, 2004, pp. 446–447.
[34] N.P.G. Roeges, A Guide to the Complete Interpretation of Infrared Spectra of Organic Structure, Wiley, New York, 1994.
[35] M. Barathes, G. De Nunzio, M. Ribet, Synth. Met. 76 (1996) 337.
[36] C. James, C. Ravikumar, T. Sundis, V. Krishnakumar, R. Kesavamoorthy, V.S. Jayakumar, I. Hubert Joe, Vib. Spectrosc. 47 (2008) 10–20.
[37] G. Socrates, Infrared Characteristic Group Frequencies, John Wiley and Sons Ltd., New York, 1980.
[38] S. Subashchandrabose, C. Meganathan, Y. Erdogdu, H. Saleem, C. Jayakumar, P. Latha, J. Mol. Struct. 1042 (2013) 37–44.
[39] N. Ramesh Babu, S. Subashchandrabose, M.S.A. Padusha, H. Saleem, Y. Erdoğdu, Spectrochim. Acta 120 (2014) 314–322.
[40] V. Krishnakumar, S. Muthunatesan, Spectrochim. Acta A 65 (2006) 818–825.
[41] P.J. Larkin, IR. Raman, Spectroscopy Principal and Spectral interpretation, Elsevier, 2011.
[42] G.D. Fleming, I. Golsio, A. Aracena, Spectrochim. Acta A71 (2008) 1049–1055.
[43] N.B. Colthup, L.H. Daly, S.E. Wiberly, Introduction to Infrared and Raman Spectroscopy, Academic Press, New York, 1990.
[44] C. Castiglioni, M. Del zoppo, P. Zuliani, G. Zerbi, Synth. Met. 74 (1995) 171–177.
[45] P. Zuliani, M. Del zoppo, C. Castiglioni, G. Zerbi, S.R. Marder, J.W. Perry, Chem. Phys. 103 (1995) 9935–9940.
[46] M. Del zoppo, C. Castiglioni, G. Zerbi, Non-Linear Opt. 9 (1995) 73.
[47] M. Del zoppo, C. Castiglioni, P. Zuliani, A. Razelli, G. Zerbi, M. Blanchard-Desce, J. Appl. Polym. Sci. 70 (1998) 73.
[48] C. Ravikumar, I. Huber Joe, V.S. Jayakumar, Chem. Phys. Lett. 460 (2008) 552–558.
[49] A.E. Reed, F. Weinhold, J. Chem. Phys. 78 (1983) 4066–4073.
[50] A.E. Reed, F. Weinhold, J. Chem. Phys. 83 (1985) 1736–1740.
[51] A.E. Reed, R.B. Weinstock, F. Weinhold, J. Chem. Phys. 83 (1985) 735–746.
[52] J.P. Foster, F. Wienhold, J. Am. Chem. Soc. 102 (1980) 7211–7218.
[53] J. Chocholousova, V. Vladimir Spirko, P. Hobza, Phys. Chem. Chem. Phys. 6 (2004) 37–41.
[54] R.M. Silverstein, F.X. Webster, Spectrometric Identification of Organic Compounds, 6th ed., Wiley, New York, 1997.